An efficient hybrid LC-S compensation topology for wireless power transfer system

Talha Irshad, Malik Nauman, Pg Emeroylariffion Abas
Faculty of Integrated Technologies, Universiti Brunei Darussalam, Brunei Muara, Brunei Darussalam

Article Info	ABSTRACT
	Wireless power transfer (WPT) system is gaining prominence for charging various applications, including electric vehicles, biomedical implants, smartphones, and network sensors. Efficient compensation networks are essential to minimize leakage inductance. The performances of single-element compensation topologies are compared based on different coupling and loading conditions, revealing that series-series (SS) and series-parallel (SP) topologies exhibit lower peak efficiencies of 85% and 90%, respectively, than parallel-series (PS) and parallel-parallel (PP) topologies, having 99% and 98.5% peak efficiency, respectively; with efficiencies deteriorating under different loading and coupling conditions. To address these shortcomings, a hybrid inductor-capacitor capacitor (LC-S) compensation topology is proposed, outperforming the single element topologies and maintaining over 95% efficiency under varying loading and coupling conditions. A slight efficiency drop to 82% due to frequency splitting was observed with low load resistance. In terms of the output characteristics, the LC-S topology achieved 1.2 W. These results showcase the potential of the LC-S topology for enhancing WPT system efficiency.

Corresponding Author:

Pg Emeroylariffion Abas
Faculty of Integrated Technologies, Universiti Brunei Darussalam
Jalan Tungku Link, Gadong A, Brunei Muara, BE1410, Brunei Darussalam
Email: emeroylariffion.abas@ubd.edu.bn

1. INTRODUCTION

Wireless power transfer (WPT) systems enable the wireless transmission of energy from source to load wirelessly. They represent a compelling alternative to conventional charging systems [1], [2], finding applications in charging electric vehicles (EVs) [3] and portable devices, including laptops and smartphones [4], and powering biomedical implants [5], [6]. Near-field electromagnetic induction techniques, including inductive and magnetic resonance coupling, play a pivotal role in WPT system design. Magnetic resonance coupling (MRC), in particular, stands out for its ability to operate with greater coupling efficiency and tolerance for misalignment when both the transmitter and receiver are tuned to the same resonance frequency [7], [8]. Hence, MRC serves as a suitable technique for the proposed WPT system, focusing particularly on applications with low power requirements, such as charging of portable devices or sensors.

The design of a WPT system often involves consideration of specific components, such as power converters (inverters and rectifiers), coils, and compensation networks tailored to a particular application. Extensive research efforts have focused on designing coil structures [9], [10], power converters, and compensation networks [4], [11]. The primary objective in developing these WPT components is to achieve optimal energy transfer efficiency, load-independent output voltage and current, and a high-quality factor. Among these components, compensation networks/topologies play a critical role in maximizing power

transfer efficiency, minimizing leak inductance (resulting from magnetic field coupling), and capacitance (related to electric field coupling) generated by the coils and capacitor plates, respectively.

Compensation topologies in WPT systems are categorized into single-resonant/single-element and multi-resonant/multi-element structures, based on reactive components. Single-element compensation topologies are developed by connecting capacitor in either parallel or series with coil inductance [12]. The four fundamental compensation topologies include series-series (SS), series-parallel (SP), parallel-series (PS), and parallel-parallel (PP) [13]-[15]. Extensive research has been conducted on various single and multi-element compensation topologies. A comparative study between SS and SP topologies aimed to optimize electric vehicle charging is given in reference [16]. Similarly, an SS topology was analyzed in comparison to a multi-element LCC topology for assessing the performance of electric vehicle wireless chargers. Both primary and secondary series or parallel compensated topologies were investigated to determine load-independent voltage transfer ratios and optimal maximum efficiency for both configurations [17].

In a basic WPT system without resonance, leakage inductance arises due to the air gap between transmitting and receiving coils, with the leakage increasing with greater coil separation [18]. To mitigate this leakage, capacitors are often introduced [19]. Together with the inductors, capacitors form resonant tanks. For efficient power transfer, the transmitter and receiver need to resonate at the same frequency, achieved through appropriate compensation on both sides, thereby reducing power leakage. The inclusion of these compensation components can enhance the power transfer efficiency (PTE) of the system. Ideally, a WPT system operates efficiently only at its resonance frequency, and to ensure efficient power transfer, current flow in the primary circuit must be minimized, necessitating the use of compensating elements such as inductors and capacitors [20].

Achieving high power transfer efficiency remains a key goal, regardless of variations in load resistance and coupling coefficient. Single-element compensation topologies often struggle to deliver high performance, especially under changing load and coupling conditions. Analysis of these single-element compensation topologies reveals that power transfer efficiency is affected by varying load and coupling conditions, as well as changes in frequency, quality factor, and coil designs. Consequently, a hybrid inductor-capacitor capacitor (LC-S) compensation topology has been proposed and compared to various single-element compensation topologies. The proposed LC-S topology offers several benefits, including zero-phase-angle operation, coupling coefficient and load-independent output. It also offers high power transfer efficiency across varying load resistances and coupling coefficients, even in the presence of resonance frequency splitting under strong coupling conditions. The remainder of the paper is organized as follows. Section 2 introduces the proposed LC-S compensation topology, its circuit model, and design analysis. Results from the simulation and comparison of the proposed topology against others are presented in section 3. Finally, section 4 concludes the work and suggests further research directions in this field.

2. METHOD

An LC-S compensation topology Figure 1(a) is proposed in this paper, consisting of a series compensation capacitor on both the primary and secondary circuits, with an additional compensation inductor on the primary side of the WPT system. The proposed topology was compared with basic single-element compensation topologies: SS, PP, PS, and SP compensation networks Figures 1(b) to (e). L_1 and L_2 represent the self-inductances of the transmitter and receiver coils, respectively, whilst C_1 and C_2 represent the compensation capacitors for the transmitter and receiver, respectively. R_L is the load resistance R_{in} is the input resistance of the primary side and V_s represents the input voltage source. L_P represents the additional compensation inductor added to the primary side of the proposed LC-S compensation topology. Figure 2 illustrates a schematic diagram depicting the structure of the transmitter and receiver coils, including the air gap and coil radii.

Self-inductance L_i of coil i ($i = 1, 2$) is determined by the number of turns N_i, the radius of wire R_i and the radius r_i of the coil i [8].

$$L_i = N_i^2 \mu_o \mu_r r_i \left[ln\left(\frac{8r_i}{R_i}\right) - 2\right], \forall i = 1,2 \tag{1}$$

where μ_o and μ_r are the permeability of free space and relative permeability, respectively. For circular coils with a gap distance of d between the transmitter and receiver coils and angle θ between the axis of the coils, mutual inductance M_{12} between the transmitter and receiver coils can then be determined using the Neumann Formula [21]:

$$M_{12} = \frac{2\mu_o N_1 N_2 \sqrt{a+b}}{b} \left[\left(1 - \frac{\beta^2}{2}\right) K(\beta) - E(\beta)\right] \tag{2}$$

where;

$$a = \frac{(r_1)^2 + (r_2)^2 + d^2}{(r_1)^2 (r_2)^2}; \quad b = \frac{2}{(r_1)(r_2)}; \quad \beta = \sqrt{\frac{2b}{a+b}} \tag{3}$$

$$K(\beta) = \int_0^{\pi/2} \left(\frac{d\theta}{\sqrt{1 - \beta^2 \sin^2 \theta}} \right); \quad E(\beta) = \int_0^{\pi/2} \left(\sqrt{1 - \beta^2 \sin^2 \theta} \, d\theta \right) \tag{4}$$
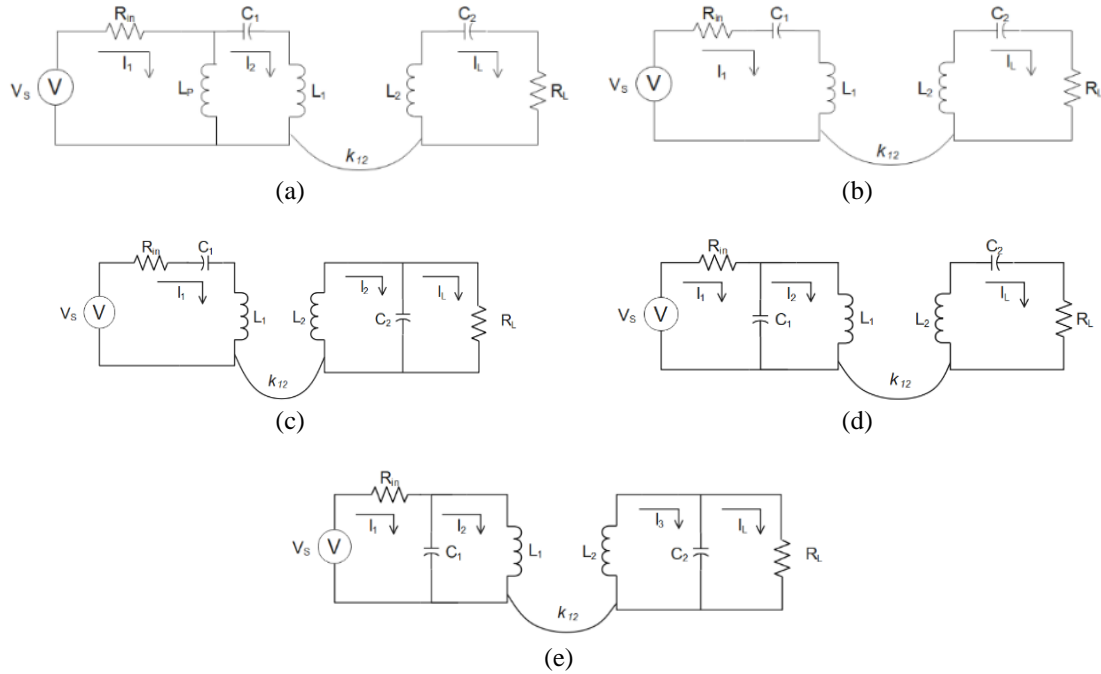
Figure 1. Schematic diagram; (a) the proposed LC-S, (b) SS, (c) SP, (d), PS, and (e) PP
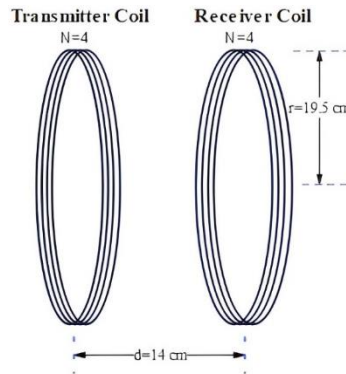
Figure 2. Schematic diagram representing the coil's structure

The coupling coefficient k_{12} between the transmitter and the receiver coils represents the rate at which the two inductive coils are magnetically coupled with each other. Generally, a large coupling coefficient results in a higher power transfer efficiency, and vice versa. It is defined as the ratio of the mutual inductance to the product of the self-inductance of two coils [22].

$$k_{12} = \frac{M_{12}}{(\sqrt{L_1 L_2})}, \quad 0 < k < 1 \tag{5}$$

For the proposed compensation network in Figure 2, the reactance of the circuit and intended resonance frequency f_o can be used to estimate the values of the compensating capacitors, C_1 and C_2 for LC-S topology,

$$C_1 = \frac{1}{(2\pi f_o)^2}\left(\frac{1}{L_p + L_1}\right) \tag{6}$$

$$C_2 = \frac{1}{(2\pi f_o)^2}\left(\frac{1}{L_2}\right) \tag{7}$$

For the single element topologies, the compensating capacitors, C_1 and C_2 are estimated using the resonance frequency and self-inductance,

$$C_1 = \frac{1}{(2\pi f_o)^2}\left(\frac{1}{L_1}\right) \tag{8}$$

$$C_2 = \frac{1}{(2\pi f_o)^2}\left(\frac{1}{L_2}\right) \tag{9}$$

Kirchhoff's voltage law can be utilized on the transmitter and receiver circuits of the proposed compensation network, to establish an expression for power transfer efficiency (η_{LC-S}),

$$\eta_{LC-S} = \frac{P_{out}}{P_{in}} = \frac{R_L|I_L|^2}{|V_sI_1|} \tag{10}$$

Given that power delivered, P_{in} by the source and the power dissipated P_{out} by the load can be derived as:

$$P_{in} = |V_sI_1| = \left[(R_{in} + \omega L_p)|I_1| - \omega L_p|I_2|\right]|I_1| \tag{11}$$

$$P_{out} = R_L|I_L|^2 = \frac{(\omega k_{12}L_p|I_1|)^2 L_1 L_2 R_L}{\left[\left(R_L + \omega L_2 - \frac{1}{\omega C_2}\right)\left(\omega L_p + \omega L_1 - \frac{1}{\omega C_1}\right) - (\omega k_{12})^2 L_1 L_2\right]^2} \tag{12}$$

Power transfer efficiency (η_{LCL-S}) for the proposed compensation topology can be expressed as:

$$\eta_{LC-S} = \frac{(\omega k_{12}L_p)^2 L_1 L_2 R_L|I_1|}{\left[(R_{in} + \omega L_p)|I_1| - \omega L_p|I_2|\right]\left[\left(R_L + \omega L_2 - \frac{1}{\omega C_2}\right)\left(\omega L_p + \omega L_1 - \frac{1}{\omega C_1}\right) - (\omega k_{12})^2 L_1 L_2\right]^2} \tag{13}$$

η_{LC-S} can be used to analyse the proposed compensation network, and its performance compared to the 4 single-element networks: SS, SP, PS and PP compensation networks.

3. RESULTS AND DISCUSSION

MRC-WPTs for single-element and the proposed hybrid LC-S compensation topologies were modelled and simulated in Keysight Advanced Design System (ADS) software. Table 1 lists the dimensions of the transmitter and receiver coils, including the radius of wire R and coil r_i, the number of turns N_i, as well as the values of the electrical parameters used, including resonance frequency f_o, input voltage V_{in}, and resistance R_{in}. Based on these parameters, self-inductance was calculated using (1), as $L_1 = L_2 = 18.3~\mu H$, to give mutual inductance $M_{12} = 2.4~\mu H$ and coupling coefficient $K_{12} = 0.13$ at a distance of $d = 14$ cm between transmitter and receiver using (2) and (3), respectively. In (8) and (9) were used to determine compensation capacitor values of $C_1 = C_2 = 62$ nF for SS, SP, PS and PP. For LC-S, primary and secondary compensation capacitors are $C_1 = 25$ nF and $C_2 = 62$ nF, respectively, determined using (6) and (7), based on compensation inductor $L_p = 26.5~\mu H$. Table 2 summarizes the values of the different components of the different compensation topologies.

Table 1. Summary of different electrical and magnetic parameters of the circuits used in the simulation

Parameter	Value
Radius r_i of coil i, $\forall i = 1,2$	19.5 cm
Radius of wire (R)	0.1 cm
Distance d between transmitter and receiver	14 cm
Permeability of free space (μ_o)	$4\pi \times 10^{-7} N/A^2$
Relative permeability (μ_r)	0.9999
Number of turns N_i of coil i, $\forall i = 1,2$	4
Resonance frequency (f_o)	150 kHz
Input resistance (R_{in})	5 Ω
Input voltage (Vs)	21.2 Vrms

Table 2. Summary of the derived components values of different compensation topologies

Parameters	Single-element network topologies				Proposed topology
	SS	SP	PS	PP	
Self-inductance $L_1=L_2$			18.3 µH		
Compensation inductor L_P		N/A			26.5 µH
Compensation capacitor C_1		62 nF			25 nF
Compensation capacitor C_2		62 nF			62 nF

Figure 3 shows the relationship between input/output power/current and load resistance R_L across various topologies. In Figure 3(a), the input power remains constant for the proposed LC-S, PP and PS topologies as load resistance R_L increases. Conversely, for the SP and SS topologies, input power decreases and increases, respectively, as higher R_L. Figure 3(b) shows that output power increases with R_L for LC-S, SP and PP topologies at $k_{12} = 0.13$, while PS and SS topologies exhibit the opposite trend. Figure 3(c) demonstrates that input current mirrors the behaviour of input power for different topologies, whilst Figure 3(d) shows output current remains constant with increasing R_L at $k_{12} = 0.13$ for LC-S and PP topologies, but decreases for PS, SS and SP topologies. The relationship between output voltage and load resistance is depicted in Figure 4; showing that as R_L increases, the output voltage rises for LC-S, PP, and SP topologies, whereas it remains constant for SS and PS topologies.
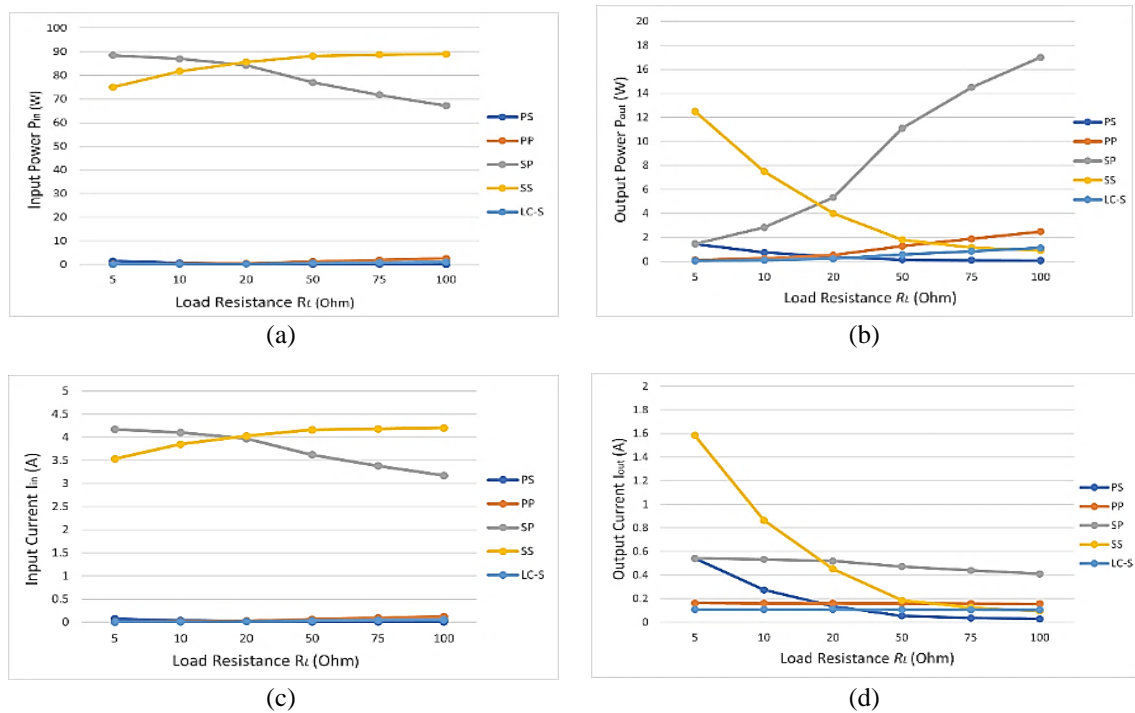

(a)   (b)

(c)   (d)

Figure 3. Load resistance for different compensation topologies at $k_{12} = 0.13$; (a) input power P_{in}, (b) output power P_{out}, (c) input current I_{in}, and (d) output current I_{out}
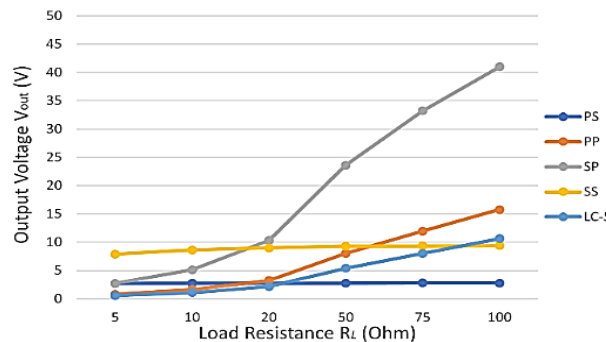

Figure 4. Output voltage against load resistance R_L for different compensation topologies

The analysis suggests that PP and LC-S topologies exhibit load-independent output current characteristics, while SS and PS topologies exhibit load-independent output voltage characteristics. To maximize efficiency, the volt-ampere (VA) rating should be minimized, as per the maximum energy efficiency principle. The analysis further indicates that SS and SP topologies have high input current and power, resulting in elevated VA ratings. Consequently, the low efficiency observed in series-compensated SS and SP topologies can be attributed to their high input-side VA ratings. The high output and input power in these series-compensated topologies stem from the high input current, which is a direct consequence of their high VA ratings, as illustrated in Figures 4(a) to (d).

Figure 5 (in Appendix) shows the relationship between efficiency and coupling coefficient k_{12} at different values of load resistance R_L, for the different compensation topologies. Power transfer efficiency decreases as coupling coefficient K_{12} increases for the proposed compensation topology, as well as the PS and PP topologies as illustrated in Figures 5(a), (d) and (e) respectively. This indicates that efficiency reduces as the distance between the transmitter and receiver of the WPT system decreases. The reverse is observed for the SS and SP compensation topologies, with efficiency increasing as the coupling coefficient is increased as shown in Figures 5(b) and (c). For both the proposed and PS topologies, power transfer efficiency slightly decreases as the coupling coefficient increases, especially with large load resistance values only. However, efficiency decreases with an increase in coupling coefficient with small load resistance values. However, it needs to be highlighted that the reduction in power transfer efficiency is less for the proposed LC-S topology as illustrated in Figure 5(a). With a load resistance value of $R_L = 100\ \Omega$, the power transfer efficiency of the proposed LC-S compensation topology is above 99% irrespective of coupling coefficient values whilst efficiency remains above 97% for the PS topology. However, efficiency reduces to 68% with a small load resistance value of $R_L = 5\ \Omega$ for the PS topology as the coupling coefficient is increased, in contrast to the proposed LC-S topology, which reduces to only 82% with a coupling coefficient of $K_{12} = 0.7$. On the other hand, efficiency considerably decreases with an increase in the coupling coefficient for the PP topology, irrespective of the size of the load resistance. These suggest that SS and SP compensation topologies are better suited for strongly coupled WPT systems, with a small distance between transmitter and receiver, whilst the PP and PS topologies can be used in loosely coupled WPT systems. The proposed topology, however, performs exceptionally well in a loosely coupled WPT system, and even in a strongly coupled system, whereby it is able to demonstrate efficiency above 80%.

In terms of variation of efficiency with load resistance, the proposed LC-S, SP and PS topologies generally exhibit higher efficiencies with larger load resistance, while the opposite trend is observed for the SS topology, where efficiency is higher with small load resistance. Peak efficiencies of approximately 99.5%, 85%, 90%, 99% and 98.5% can be achieved with the proposed LC-S, SS, SP, PS and PP topologies, respectively. Specifically, the LC-S topology reaches a peak efficiency of 99.5% with $R_L = 100\ \Omega$ and $K_{12} = 0.13$, closely followed by the PS topology, with 99% efficiency under the same conditions. Notably, even at the lowest observed efficiency for the LC-S topology, it still maintains 82% efficiency with $R_L = 5\ \Omega$ and $K_{12} = 7$; representing a modest 17.5% reduction compared to the other topologies. Efficiencies of the LC-S, PS, and PP topologies are extremely close to 100%, as the circuit designs were kept simple to minimize losses. It is also important to note that the analysis does not account for inverter and rectifier losses.

Table 3 provides a summary of the efficiencies along with relevant parameters, including input voltage V_{in}, output power P_{out}, load resistance R_L and coupling coefficient K_{12} of the proposed LC-S topology alongside various single-element and hybrid topologies from the literature. The findings show that the LC-S topology offers comparable performance to other hybrid topologies, such as S/SP topology with a maximum efficiency of 95% and load independent output voltage characteristics [23], as well as a similar three-coil hybrid SSLCC topology with a maximum efficiency of 90% [24]. The LC-S topology achieves a peak output power of 1.2 W while the SS, SP, PS and PP topologies reach peak output powers of 12.5 W, 17 W, 1.8 W and 2.5 W, respectively. The higher output power of series SS and SP topologies is attributed to their elevated input power (VA rating), as shown in Figure 4(a). Similarly, hybrid topologies such as S/SP and LCC-LCC exhibit peak output powers of 1.5 kW and 3.1 kW, with input voltages of 528 V and 359 V, respectively. The comparison clearly demonstrates that despite its low output power and coupling coefficient, the proposed LC-S topology outperforms both single element and hybrid compensation topologies in terms of efficiency.

Figure 6 depicts the relationship between efficiency and operating frequency at various load resistances for the proposed LC-S compensation topology. The LC-S topology exhibits the frequency splitting/bifurcation phenomenon at low load resistance $R_L = 5\ \Omega$ (Figure 6(a)), particularly as the coupling coefficient k_{12} is increased. The resonance frequency splits into two halves at $k_{12} = 0.70$; with the low and high-frequency peaks occurring at 128 kHz and 198 kHz, respectively. The frequency splitting does not occur with large load resistances as illustrated in Figures 6(b) and (c). The frequency splitting partly explains the observed reduction in power transfer efficiency with low load resistance as the coupling coefficient is

increased in Figure 4. The result also indicates that the resonance frequency of the proposed LC-S topology is independent of the coupling coefficient at relatively large load resistance values.

Table 3. PTE and corresponding parameters of the different compensation topologies

| Parameters	Single-element topologies				Proposed topology	Different hybrid topologies			
	SS	SP	PS	PP		S/SP [23]	LCL-LCL [25]	LCC-LCC [20]	LCC-S [20]
Peak power transfer eff. (%)	85	90	99	98.5	99.5	95.2	95.87	93.5	94.2
K_{12} at peak efficiency	0.7	0.7	0.13	0.13	0.13	0.475	0.222	0.182	0.182
R_l at peak efficiency (Ω)	5	100	100	50	100	800	36	N/a	N/a
Lowest power transfer eff. (%)	2	3	67.5	53	82	N/A			
Var. in efficiency from peak eff (%)	-83	-87	-31.5	-45.5	-17.5	N/A			
Input voltage v_{in} (v)			21.2			528	N/a	350	350
Resonance frequency (kHz)			150			40	20	85	85
Output power (p_{out})	12.5 w	17 w	1.8 w	2.5 w	1.2 w	1.5 kw	7.3 kw	3.1 kw	3.1 kw
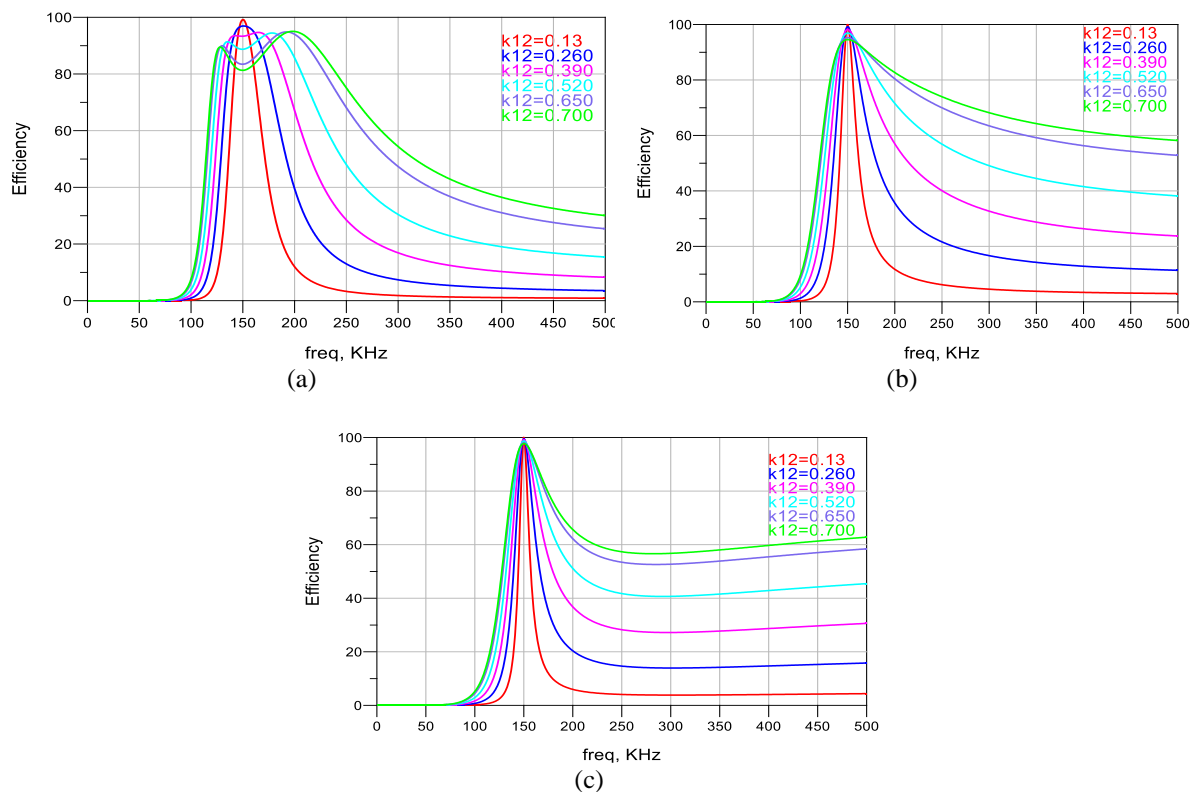
Figure 6. PTE against frequency for the proposed LC-S compensation topology with different load resistances; (a) $R_L = 5$ Ω, (b) $R_L = 20$ Ω, and (c) $R_L = 50$ Ω

4. CONCLUSION

WPT faces efficiency challenges as coupling coefficient fluctuates due to misalignment and changes in transmitter-receiver distance during charging. Additionally, load resistance may also change with different applications. To address these issues, a hybrid LC-S compensation topology was introduced, demonstrating superior performance compared to single-element topologies. The LC-S topology achieved exceptional

power transfer efficiency across diverse load resistances and coupling conditions, peaking 99.5% and consistently exceeding 95%. Frequency splitting resulted in a minor drop to 82% efficiency with low load resistance. In contrast, the SS and SP topologies reached only 85% and 90% efficiency, respectively, with the efficiency dropping below 10 % with significant load variations. Similarly, the PS and PP topologies achieved peak efficiencies of 99% and 98.5%, respectively, and experienced significant drops with changing loads. On the other hand, the LC-S topology displayed greater resilience to efficiency loss despite minor decreases with low load resistance. These findings underscore the adaptability of the LC-S topology in both strongly and loosely coupled WPT systems, particularly effective with large load resistance and modest coupling coefficients. This research contributes to enhancing WPT system performance, with future work focused on constant current and constant voltage characteristics, as well as topology fabrication and testing within operational WPT systems.
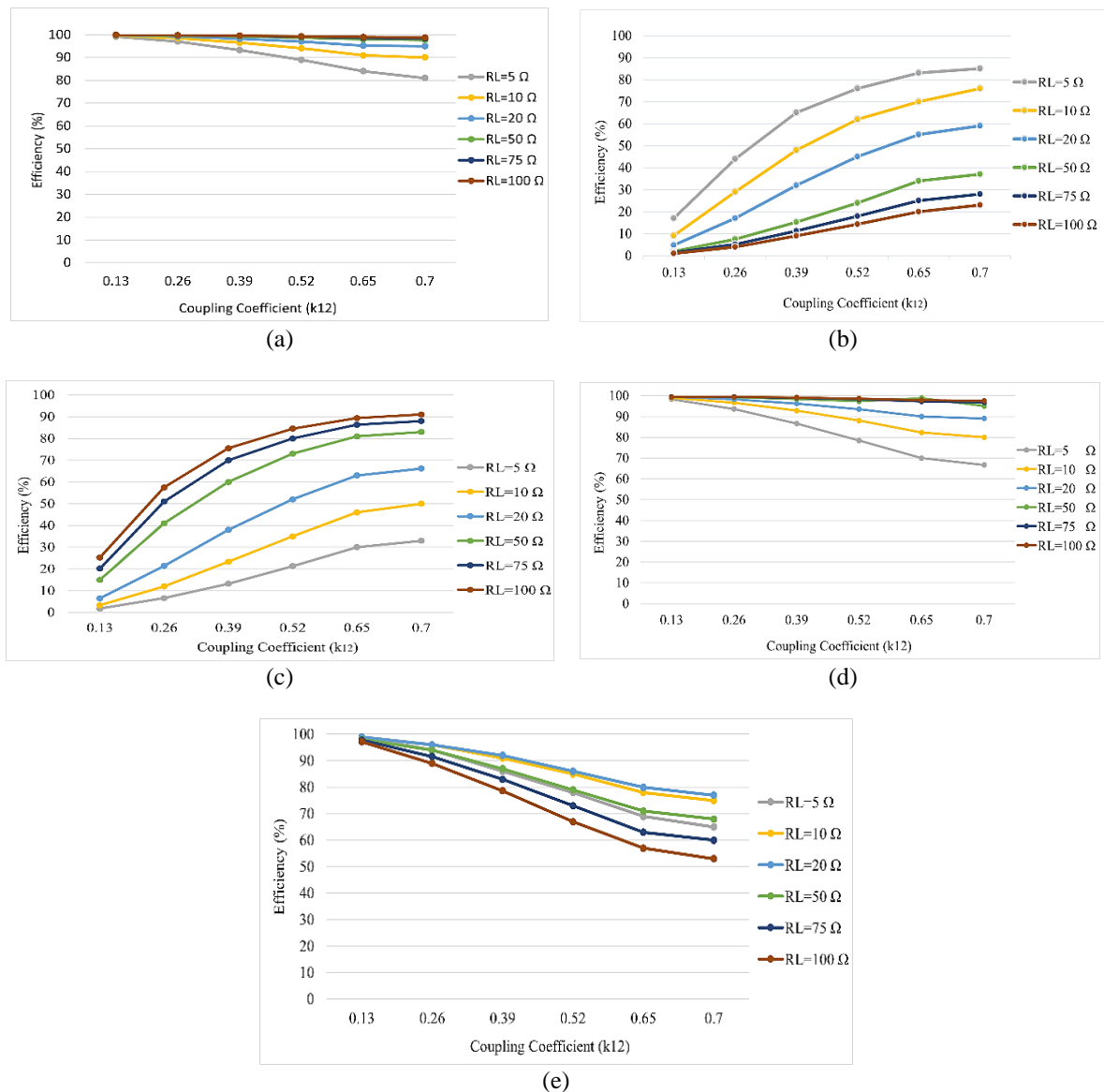
APPENDIX

(a)   (b)

(c)   (d)

(e)

Figure 5. PTE against coupling coefficient *(k)* and load resistance for different compensation topologies; (a) the proposed LC-S, (b) SS, (c) SP, (d) PS, and (e) PP

REFERENCES

[1] A. I, Mahmood, S. K. Gharghan, M. A. Eldosoky, and A. M. Soliman, "Wireless charging for cardiac pacemakers based on class-D power amplifier and a series–parallel spider-web coil," *International Journal of Circuit Theory and Applications*, vol. 51, no. 1, pp. 1–17, Sep. 2022, doi: 10.1002/cta.3420.

[2] Z. Zhang, H. Pang, A. Georgiadis, and C. Cecati, "Wireless Power Transfer—An Overview," *IEEE Transactions on Industrial Electronics*, vol. 66, no. 2, pp. 1044–1058, 2019, doi: 10.1109/tie.2018.2835378.

[3] M. Venkatesan *et al.,* "A Review of Compensation Topologies and Control Techniques of Bidirectional Wireless Power Transfer Systems for Electric Vehicle Applications," *Energies*, vol. 15, no. 20, 2022, doi: 10.3390/en15207816.

[4] J. Feng, Q. Li, and F. C. Lee, "Coil and Circuit Design of Omnidirectional Wireless Power Transfer System for Portable Device Application," *IEEE Energy Conversion Congress and Exposition (ECCE),* pp. 914–920, 2018, doi: 10.1109/ECCE.2018.8557465.

[5] C. Kim *et al.,* "Design of miniaturized wireless power receivers for mm-sized implants," *2017 IEEE Custom Integrated Circuits Conference (CICC),* Austin, TX, USA, 2017, pp. 1-8, doi: 10.1109/CICC.2017.7993703.

[6] K. M. Silay *et al.,* "Load Optimization of an Inductive Power Link for Remote Powering of Biomedical Implants," *2009 IEEE International Symposium on Circuits and Systems*, pp. 533–536, 2009, doi: 10.1109/ISCAS.2009.5117803.

[7] S. D. Barman, A. W. Reza, N. Kumar, Md. E. Karim, and A. B. Munir, "Wireless powering by magnetic resonant coupling: Recent trends in wireless power transfer system and its applications," *Renewable and Sustainable Energy Reviews*, vol. 51, pp. 1525–1552, 2015, doi: 10.1016/j.rser.2015.07.031.

[8] M. A. Houran, X. Yang, and W. Chen, "Magnetically coupled resonance wpt: Review of compensation topologies, resonator structures with misalignment, and emi diagnostics," *Electronics,* vol. 7, no. 11, pp. 1–45, 2018, doi: 10.3390/electronics7110296.

[9] M. A. Houran, X. Yang, W. Chen, and X. Li, "Design and analysis of coaxial cylindrical WPT coils for two-degree-of-freedom applications," *Journal of Physics D: Applied Physics*, vol. 53, no. 49, p. 495004, Oct. 2020.

[10] M. A. Houran, X. Yang, and W. Chen, "Two-Degree-of-Freedom WPT System Using Cylindrical-Joint Structure for Applications with Movable Parts," *IEEE Transactions on Circuits and Systems II: Express Briefs*, vol. 68, no. 1, pp. 366–370, Jan. 2021, doi: 10.1109/TCSII.2020.2995616.

[11] P. Darvish, S. Mekhilef, S. Member, H. Azil, B. Illias, and S. Member, "A Novel S-S-LCLCC Compensation for Three-Coil WPT to Improve Misalignment and Energy Efficiency Stiffness of Wireless Charging System," *IEEE Transactions on Power Electronics*, vol. 8993, no. c, 2020, doi: 10.1109/TPEL.2020.3007832.

[12] Y. Wang, Y. Yao, X. Liu, D. Xu, and L. Cai, "An LC/S Compensation Topology and Coil Design Technique for Wireless Power Transfer," *IEEE Transactions on Power Electronics*, vol. 33, no. 3, pp. 2007–2025, Mar. 2018, doi: 10.1109/TPEL.2017.2698002.

[13] B. A. Rayan, U. Subramaniam, and S. Balamurugan, "Wireless Power Transfer in Electric Vehicles: A Review on Compensation Topologies, Coil Structures, and Safety Aspects," *Energies*, vol. 16, no. 7, Apr. 01, 2023. doi: 10.3390/en16073084.

[14] K. N. Mude and K. Aditya, "Comprehensive Review and Analysis of Two-element Resonant Compensation Topologies for Wireless Inductive Power Transfer Systems," *Chinese Journal of Electrical Engineering*, vol. 5, no. 2, pp. 14–31, 2019, doi: 10.23919/CJEE.2019.000008.

[15] A. Agcal, S. O. Ozkilic, and K. Toraman, "Comparison and selection strategy among compensating topologies in two-coil resonant wireless power transfer systems," *Journal of Engineering Research*, vol. 11, no. 2, pp. 148–157, Jun. 2023, doi: 10.36909/jer.14245.

[16] K. Aditya and S. S. Williamson, "Comparative study of Series-Series and Series-Parallel compensation topologies for electric vehicle charging," *2014 IEEE 23rd International Symposium on Industrial Electronics (ISIE),* pp. 426–430, 2014, doi: 10.1109/ISIE.2014.6864651.

[17] W. Zhang, S. -C. Wong, C. K. Tse and Q. Chen, "Analysis and Comparison of Secondary Series- and Parallel-Compensated Inductive Power Transfer Systems Operating for Optimal Efficiency and Load-Independent Voltage-Transfer Ratio," in *IEEE Transactions on Power Electronics*, vol. 29, no. 6, pp. 2979-2990, June 2014, doi: 10.1109/TPEL.2013.2273364.

[18] S. Li, W. Li, S. Member, J. Deng, and S. Member, "A Double-Sided LCC Compensation Network and Its Tuning Method for Wireless Power Transfer," *IEEE Transactions on Vehicular Technology*, vol. 64, no. 6, pp. 2261–2273, 2015, doi: 10.1109/TVT.2014.2347006.

[19] M. Rehman, P. Nallagownden, and Z. Baharudin, "Efficiency investigation of SS and SP compensation topologies for wireless power transfer," *International Journal of Power Electronics and Drive System (IJPEDS),* vol. 10, no. 4, pp. 2157–2164, 2019, doi: 10.11591/ijpeds.v10.i4.pp2157-2164.

[20] W. Zhang, and C. C. Mi, "Compensation Topologies of High-Power Wireless Power Transfer Systems," *IEEE Transactions on Vehicular Technology*, vol. 65, no. 6, pp. 4768–4778, 2016, doi: 10.1109/TVT.2015.2454292.

[21] K. Nalty, "Classical calculation for mutual inductance of two coaxial loops in MKS units," *YUMPU*, pp. 1–8, 2011, [Online] Available: https://51.158.55.107/en/document/view/37761616/classical-calculation-for-mutual-inductance-of-two-kurt-nalty?__cpo=aHR0cHM6Ly93d3cueXVtcHUuY29t.

[22] V. Jiwariyavej, T. Imura, and Y. Hori, "Coupling coefficients estimation of wireless power transfer system via magnetic resonance coupling using information from either side of the system," *IEEE Journal of Emerging and Selected Topics in Power Electronics*, vol. 3, no. 1, pp. 191–200, 2015, doi: 10.1109/JESTPE.2014.2332056.

[23] J. Hou, Q. Chen, S. C. Wong, C. K. Tse, and X. Ruan, "Analysis and control of series/series-parallel compensated resonant converter for contactless power transfer," *IEEE Journal of Emerging and Selected Topics in Power Electronics*, vol. 3, no. 1, pp. 124–136, Mar. 2015, doi: 10.1109/JESTPE.2014.2336811.

[24] Y. Li, Q. Xu, T. Lin, J. Hu, Z. He, and R. Mai, "Analysis and design of load-independent output current or output voltage of a three-coil wireless power transfer system," *IEEE Transactions on Transportation Electrification*, vol. 4, no. 2, pp. 364–375, 2018, doi: 10.1109/TTE.2018.2808698.

[25] C. Liu, S. Ge, Y. Guo, H. Li, and G. Cai, "Double-lcl resonant compensation network for electric vehicles wireless power transfer: Experimental study and analysis," *IET Power Electronics*, vol. 9, no. 11, pp. 2262–2270, 2016, doi: 10.1049/iet-pel.2015.0186.

BIOGRAPHIES OF AUTHORS

Talha Irshad received a BS degree in Electronic Engineering from Capital University of Science and Technology, Pakistan, in 2016 and an MS degree in electrical and electronic engineering from Universiti Sains Malaysia, Pulau Pinang, Malaysia, in 2020. Currently, he is a Ph.D. candidate at the Faculty of Integrated Technologies, Universiti Brunei Darussalam. His research interests include wireless power transfer, power electronics, wireless charging, and compensation topologies for wireless power transfer. He can be contacted at email: 21h8452@ubd.edu.bn.

Malik Nauman is an accomplished academic and researcher with over 11 years of experience in Manufacturing, Energy Engineering, and Innovation and Entrepreneurship. He has worked in various universities across the globe, including in Turkey and Saudi Arabia, before joining the Faculty of Integrated Technologies at Universiti Brunei Darussalam as an Associate Professor and Deputy Dean. His research expertise extends beyond energy devices and encompasses other areas, such as image processing and shape memory alloys. He has published numerous research papers and articles in reputed international journals and conferences in these fields. He can be contacted at email: malik.nauman@ubd.edu.bn.

Pg Emeroylariffion Abas received his Bachelor of Engineering in Information System Engineering from Imperial College, London in 2001, before obtaining his PhD in Communication Systems in 2005 at the same institution. After working as an engineer for several years, he joined academia in 2015. He is currently and Senior Assistant Professor in Information System Engineering at the Faculty of Integrated Technologies, Universiti Brunei Darussalam. His present research interests include data analytics, techno-economic analysis, and photonics. He can be contacted at email: emeroylariffion.abas@ubd.edu.bn.